https://doi.org/10.1016/j.ijhydene.2017.03.229

A high performance direct carbon solid oxide fuel cell fueled by Ca-loaded activated carbon

Weizi Cai[a,b], Jiang Liu[a,*], Fangyong Yu[a,c], Qian Zhou[a], Yapeng Zhang[a], Xiaoqiang Wang[a], Meilin Liu[a,d], Meng Ni[b,*]

[a] New Energy Research Institute, School of Environment and Energy, South China University of Technology, Guangzhou 510006, P.R. China.

[b] Building Energy Research Group, Department of Building and Real Estate, The Hong Kong Polytechnic University, Hung Hom, Kowloon, Hong Kong 999077, P. R. China.

[c] School of Chemical Engineering, Shandong University of Technology, Zibo, Shandong 255049, P. R. China.

[d] School of Materials Science and Engineering, Georgia Institute of Technology, 771Ferst Drive, Atlanta, GA 30332-0245, USA.

Abstract

Ca-loaded activated carbon is developed as fuel for direct carbon solid oxide fuel cells (DC-SOFCs), operating without any carrier gas and liquid medium. Ca is loaded on activated carbon through impregnation technique in the form of CaO, which exhibits excellent catalytic activity and significantly promotes the output performance of DC-SOFCs. DC-SOFCs fueled by activated carbon with different Ca loading content (0, 1, 3, 5 and 7 wt. %) are tested and the performances are compared with the DC-SOFC

*Corresponding author:
Tel.: +86 20 22236168, Fax: +86 20 22236168, E-mail: jiangliu@scut.edu.cn(Prof. J. LIU)
Tel.: +852 27664152, Fax: +852-27645131, Email: bsmengni@polyu.edu.hk (Prof. M. NI)

running on the conventional Fe-loaded activated carbon. It is found that the performance of the DC-SOFC with 5 wt. % (373 mW cm^{-2}) and 7 wt.% (378 mW cm^{-2}) Ca-loaded activated carbon is significantly higher than that of the cells operated on 5 wt.% Fe-loaded activated carbon, 1 wt.% and 3 wt.% Ca-loaded activated carbon. The discharging time and fuel utilization of the DC-SOFC with 5 wt. % Ca-loaded activated carbon are also the optimal ones among all the cells. The microstructure, element distribution and carbon conversion rate of the Ca-loaded carbon, the impedance spectra of the corresponding DC-SOFCs are measured. The reasons for the reduced fuel utilization of 7 wt. % Ca-loaded carbon fuel are analyzed and the advantage of Ca-loaded carbon for DC-SOFCs is demonstrated in detail.

Keywords: Solid oxide fuel cells, Carbon fuel, Ca catalyst, Boudouard reaction

1. Introduction

Currently, fossil fuel is still the major energy source in the world, contributing to 80% of the global primary energy supply [1]. Coal, as the major part of fossil fuels, is abundant and widely available, especially in China [2]. However, the conversion efficiency of conventional coal-fired power plants is relatively low and very difficult to further enhance, due to the limitations of the Carnot cycle. Recently, direct carbon fuel cell (DCFC) has received considerable attention for energy conversion from carbon to electricity, because of its high energy efficiency, environment friendliness and high fuel

utilization [3-10]. Unlike the conventional heat engines, direct carbon fuel cell is not limited by Carnot cycle [3]. Benefitting from the abundant carbon sources and lower CO_2 emissions, DCFC offers advantages of low cost of fuel and less environment impact [11]. Therefore, DCFC might be a promising future power generating technology, as well as a clean coal technology [12-15].

Direct carbon solid oxide fuel cell (DC-SOFC) is a kind of DCFCs with whole solid state configuration, without carrier gas or liquid medium [16-22]. As early as 1988, Nakagawa and Ishida [16] designed a DC-SOFC without any liquid medium and proposed the mechanism of a DC-SOFC as the coupling of electrooxidation of CO on the anode (1) and the Boudouard reaction on the surface of carbon (2).

$$CO + O^{2-} \rightarrow CO_2 + 2e^- \quad (1)$$

$$CO_2 + C \rightarrow 2CO \quad (2)$$

As the electrochemical characteristics of the cells operating on CO and solid carbon are exactly the same, Xie et.al. verified this mechanism indirectly [21]. Therefore, catalyzing the carbon gasification reaction (the Boudouard reaction) is a simple and effective way to improve the DC-SOFC performance [18, 23, 24]. Iron is one of the efficient catalysts. Tang et. al. demonstrated that the use of Fe catalyst for Boudouard reaction could enhance the performance of DC-SOFCs [18]. Later on, a Ni-YSZ anode-supported SOFC stack fueled by 5 wt. % Fe-loaded activated carbon was developed and yielded a peak power density of 465 mW cm^{-2} at 850 ºC [20]. Similarly, Skrzypkiewicz et. al. investigated DC-SOFCs operated on Fe_2O_3-loaded carbon fuels.

With Fe_2O_3-loaded carbon, the DC-SOFC delivered a peak power density of 152 mW cm^{-2} at 850 ºC [25] . Other Boudouard reaction catalysts, like Li, K, Ni and Ca (10 wt. %), were also investigated to promote the DCFC performance [11, 23]. However, compared to a hydrogen fueled SOFC (over 1000 mW cm^{-2}, at 800 ºC), the performance of DC-SOFC (424 mW cm^{-2}, at 850 ºC) [20] is still unsatisfactory. Therefore, to enhance the output performance and fuel utilization of DC-SOFCs, it is necessary to develop more effective catalysts for carbon fuel in DC-SOFCs.

In this work, we report a high performance Ca-loaded activated carbon DC-SOFC, with good fuel utilization. Through the impregnation method, Ca is loaded on the activated carbon in the form of CaO, similar to the conventional Fe-loaded activated carbon for DC-SOFCs. The performances of the DC-SOFCs operated on carbon fuels with different Ca loading content (1-7 wt. %) are compared with that of the DC-SOFC with Fe-loaded (5 wt. %) carbon fuel. The microstructure, element distribution and carbon conversion rate of the Ca-loaded carbon, the impedance spectra of the corresponding DC-SOFCs are measured. The reason for the reduced fuel utilization of 7 wt. % Ca-loaded carbon fuel is analyzed and the advantage of Ca-loaded carbon for DC-SOFCs is demonstrated in detail.

2. Experimental

2.1. Pre-treatment of carbon fuels

Pure activated carbon powders were prepared by crushing activated carbon

84 granules (Activated Charcoal, 8-16 mesh, Aladdin) using an electric grinder, followed
85 by sieving through a sieve (77 mesh). Six kinds of carbon fuel were prepared (Table 1).
86 1 wt. %, 3 wt. %, 5 wt. %, 7 wt. % of Ca and 5 wt. % Fe catalyst was loaded on the
87 pure activated carbon powders by impregnation technique, which had been reported
88 previously [18, 20, 23]. $Ca(NO_3)_2 \cdot 4H_2O$ and $Fe(NO_3)_3 \cdot 9H_2O$ were dissolved in purified
89 water with a slight stirring, respectively. Under stirring, the pure activated carbon
90 powders were added into the $Ca(NO_3)_2$ and $Fe(NO_3)_3$ solutions. After stirring for 1 h,
91 the mixtures were heated at 80 ºC till the solvent was evaporated. Afterwards, to
92 decompose the nitrate, the catalyst-loaded carbon fuels were placed in a tubing oven,
93 followed by heating at 700 ºC for 1 h under N_2 atmosphere. After heat-treatment,
94 $Ca(NO_3)_2$ and $Fe(NO_3)_3$ decompose into CaO and Fe_2O_3, depositing on the surface of
95 activated carbon. The form of CaO and Fe_2O_3 have been confirmed by the XRD of Ca-
96 loaded activated carbon before cell operation (Fig. S1 in the supplementary material)
97 and our previous work [26], respectively.
98
99 **Table 1 – Activated carbon fuels with different catalyst and the performances of**
100 **the corresponding DC-SOFCs operated on these carbon fuels at 850 ºC.**

	C-1	C-2	C-3	C-4	C-5	C-6
Catalyst	1 % Ca	3 % Ca	5 % Ca	7 % Ca	5 % Fe	none
Open circuit voltage/ V	0.96	0.98	1.0	1.01	0.96	0.92
Maximum power density/ mW cm^{-2}	324	358	373	378	352	258
Polarization resistance/ Ω cm^2	0.123	0.099	0.095	0.092	0.109	0.164

2.2. Fabrication of SOFCs

Electrolyte-supported button cells were fabricated and tested in this study. To improve the ionic conductivity of electrolyte, 1 wt. % alumina powder was added into Yttria-stabilized-zirconia (YSZ, TZ-8Y, Tosoh Corporation, Tokyo, Japan) [27, 28]. First, YSZ powder and alumina powder (Al_2O_3, Xinfumeng, China, α-phase, 99.99 % purity) were mixed by wet ball-milling for 3 hours with zirconia balls as milling medium and alcohol as solvent, followed by drying the solvent under an infrared lamp. Then, electrolyte disks were prepared by uni-axial pressing of the Al_2O_3-added-YSZ powders into pellets (each of 0.15 g in weight and 13 mm in diameter). After that, the pellets were sintered at 1400 ºC for 4 hours in air atmosphere. The dense electrolyte pellets were about 300 μm in thickness and 11 mm in diameter. Ag-GDC is chosen to be the materials of anode and cathode, because silver and GDC are not only effective catalysts for electrochemical oxidation of CO, but also excellent anode materials for their high oxygen ion conductivity and electron conductivity [29], which are suitable for DC-SOFC [18]. To prepare anode and cathode, a Ag/GDC slurry was prepared by mixing 37 wt. % silver paste (DAD-87, with 80 wt. % Ag, Shanghai Research Institute of Synthetic Resins, Shanghai, China), 13 wt.% GDC ($Gd_{0.1}Ce_{0.9}O_{2-\delta}$, purity ≥ 99.5%, particle size (d50): 0.5-3 μm, Ningbo Institute of Materials Technology & Engineering, China) and 50 wt.% polyvinyl butyral alpha-terpineol solution (weight concentration: 10 %) by grinding in an agate mortar for about 3 hours until the slurry was uniform. Afterward, the resulting slurry was painted onto both sides of the electrolyte disks, and

then annealed at 880 ºC in air for 4 hours. The cathode area was controlled to be 0.22 cm^2, using a mask with a hole in the middle. Finally, SOFCs with a configuration of Ag-GDC/YSZ/Ag-GDC were obtained.

2.3. Cell assembling and characterization

In order to test the SOFCs, silver paste was used as sealing and jointing materials to connect the cells to one end of an alumina tube. Silver wires were attached to the anode and cathode, and connected to an Iviumstate electrochemical analyzer (Ivium Technologies B.V., Netherlands). A SOFC operated on humidified hydrogen (3 vol.% H_2O) was first tested to evaluate the performance of the typical as-prepared SOFCs. The H_2 gas flow rate was 30 mL min^{-1}. For the cells operated on solid carbon fuels, including the five catalyst-loaded activated carbon fuels and pure activated carbon, 0.4 g carbon was filled into each cell. For the other end of the alumina tube, a rubber stopper with a plastic gas-guide pipe was used to block, and leading the emitted gas out. In all testing, the cathode side was exposed to ambient air (Fig. 1). An alternating current voltage perturbation of 10 mV was applied in equilibrium within a frequency range of 0.1- 10^5 Hz to measure the impedance of the cells. The microstructures of the SOFCs and EDX were characterized by a scanning electron microscope (SEM, Carl Zeiss AG-Merlin, Germany). The reactivity of all the catalyst-loaded carbon fuel in this experiment is investigated under programmed-temperature conditions using a Thermogravimetric analyzer (TGA, Mettler Toledo, Swizerland). In each gasification

experiment, 4-5 mg of carbon fuel was loaded in ceramic pan under a flowing N_2 atmosphere with a flow rate of 50 ml min^{-1} and a heating rate of 20 ºC min^{-1} from 25 ºC to 850 ºC. After the temperature reached 850 ºC, the atmosphere was switched to CO_2 (50 ml min^{-1}). X-ray diffraction (XRD, Rigaku D/max-IIIA diffractometer, Japan, Cu-Ka radiation, operated at 35 kV, 30 mA, l = 1.54184 Å) was performed on the Ca-loaded carbon fuel before and after discharging process.

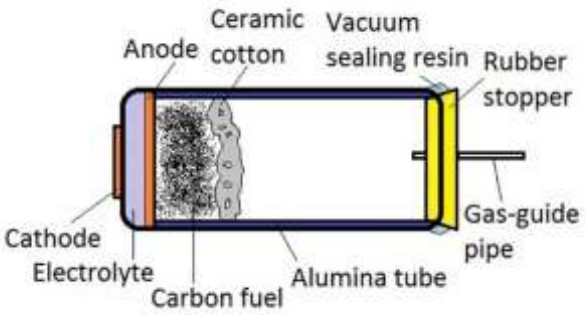

Fig. 1 – Schematic diagram of a DC-SOFC.

3. Results and discussion

3.1. Characteristics of the as-prepared SOFCs

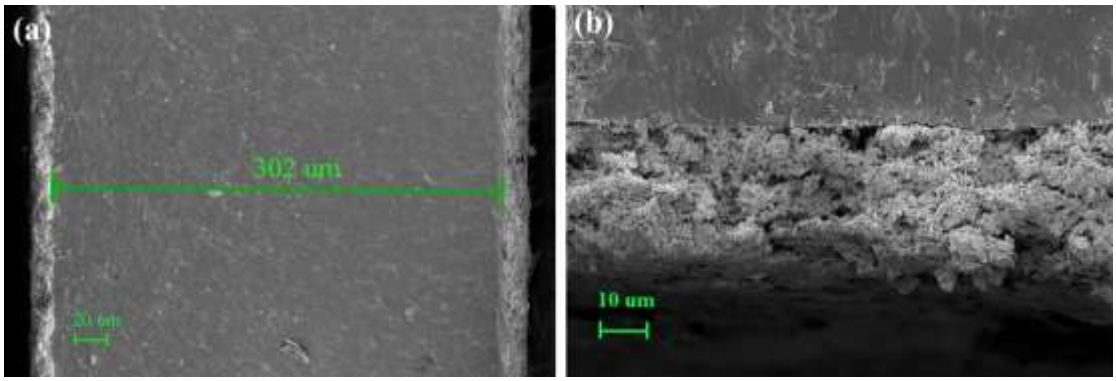

Fig. 2 – SEM pictures of cross-section (a, scale: 300) and anode (b, scale: 1000) of the as prepared SOFC.

The microstructures of the as prepared SOFCs are shown in Fig. 2. From the section image (Fig. 2a), we can see that the YSZ electrolyte is quite dense, only with some closed pores which will not affect the gas tightness of the cell. The thickness of the YSZ electrolyte is about 300 μm. The anode layer, with a thickness of 20 μm, closely attaches to the YSZ electrolyte substrate. The surface image of the anode (Fig. 2b) shows that the anode is fairly porous with relatively uniform microstructure.

To evaluate the performance of a SOFC, the power output curve and impedance spectra of a typical as-prepared SOFC operated at 850 ºC, with humidified H_2(3 vol.% H_2O) as fuel, are measured. As shown in Fig.3 (a), an open circuit voltage of 1.05 V and a maximum power density of 404 mW cm^{-2} are obtained, showing that the SOFCs are well prepared. The high linearity of I-V curve is caused by the high electrolyte resistance of DC-SOFC, and the cathode contribution is overshadowed.

The errors are calculated through the standard deviation of the data. In the experiment, we controlled the voltages and measured the corresponding currents. Hence the voltages are represented in X-axis and currents Y-axis in Fig. 3 (a). As we can see, the performance errors of the hydrogen cells are very small, indicating that the quality of the as-prepared cells is reliable.

Fig.3 (b) is the impedance spectrum of the SOFC under open circuit voltage. As we know, the intercept of the real axis at high-frequency, which represents the ohmic resistance of the cell, is about 0.53 Ω cm^2. The low frequency intercept with the real

axis represents the overall resistance of the cell, which is 0.61 Ω cm^2. Therefore, the polarization of the H_2 fuelled SOFC is 0.08 Ω cm^2 (0.61-0.53=0.08 Ω cm^2).

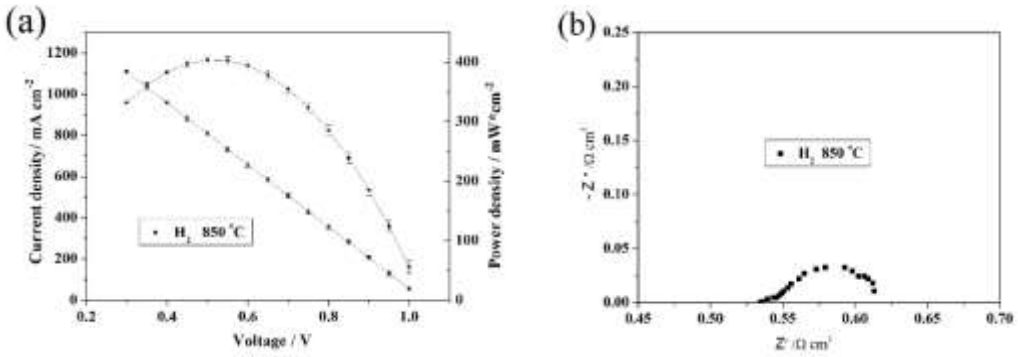

Fig. 3 – The output performance plot with error bars (a) and impedance spectra (b) of a typical as-prepared SOFC operated at 850 ºC using H_2 as fuel gas.

3.2. Characterizations of carbon fuels

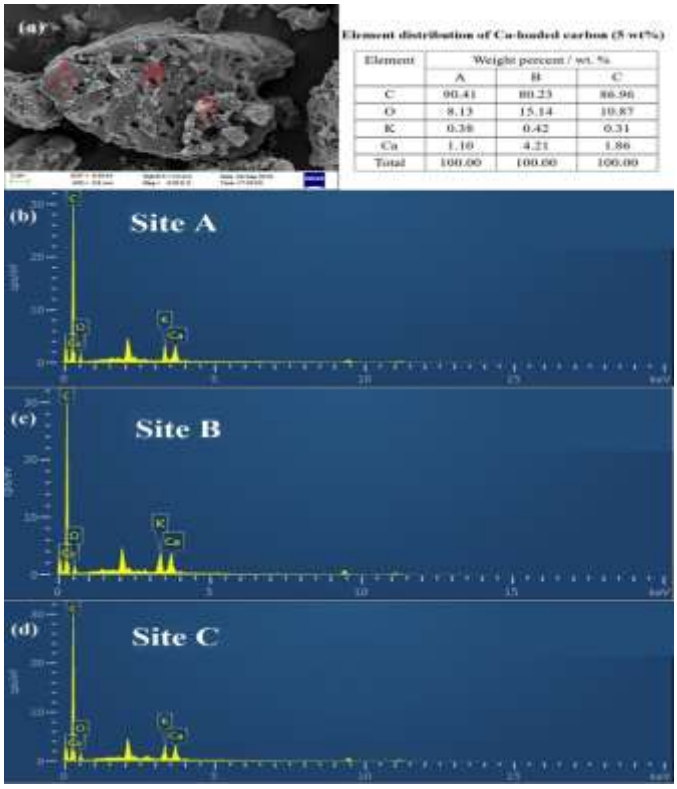

Fig. 4 – SEM image (a) and EDX diagrams of the Ca-loaded activated carbon fuel (5 wt. %) on different sites.

The microstructure and EDX spectra of Ca-loaded activated carbon fuel on different site are shown in Fig. 4. The surface of the carbon particle is rough with some pores in the bulk, which explains its large surface area. The existence of Ca element of carbon is verified by the EDX measurement. However, the amount of Ca element on smooth surface (site A) is lower than that on holes (site B) and rough surface (site C). It might be caused by the capillary action. The Ca catalyst is loaded on carbon using $Ca(NO_3)_2$ aqueous solution as Ca source by impregnation method. Holes on carbon particle provide a room to store $Ca(NO_3)_2$ aqueous solution, resulting a higher Ca content on holes and portals. Furthermore, the different distribution of oxygen-containing functional groups on carbon particle might result in the different distribution of Ca catalyst, as the functional groups have a strong adsorption force to metal ions. In addition, the peaks in the EDX diagrams (2.1, 2.2 and 9.5 keV) is attributed to Au, which is a conductive additive to increase the electron conductivity of the sample in scanning electron microscope.

3.3. Electrochemical performance of DC-SOFCs

In a DC-SOFC, CO is formed through the Boudouard reaction (2) on the carbon fuel and electrochemically oxidized on the anode of the cell (reaction 1) [21]. From reaction (1), the electrochemical oxidation of CO generates the same molar amount of CO_2, which would diffuse to the carbon fuel and participate in the Boudouard reaction.

As a result, the OCV and output performance of a DC-SOFC are controlled by the concentration of CO, according to the Nernst equation. However, the concentration of CO is highly dependent on the Boudouard reaction, indicating that the Boudouard reaction directly influences the electrochemical performance of a DC-SOFC. Therefore, the performance of a DC-SOFC operated on carbon fuel can be substantially enhanced by loading Fe catalyst on carbon to facilitate the Boudouard reaction. So far, one of the best reported DC-SOFCs performances has been achieved using 5 wt. % Fe-loaded activated carbon, as shown in Fig. 5a (C-5, 5 wt. % Fe).

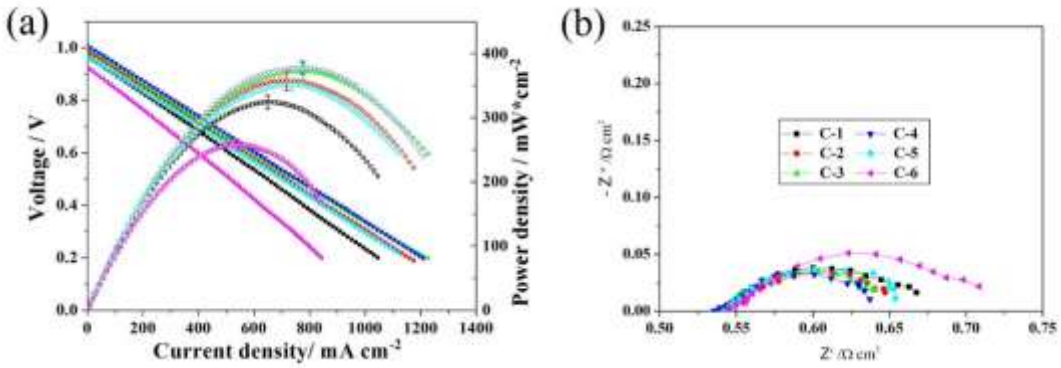

Fig. 5 – I-V-P characteristics (a) with error bars and impedance spectra (b) of the SOFCs operated at 850 °C using the different kinds of catalyst-loaded carbon fuel (C-1, 1 wt.% Ca; C-2, 3 wt.% Ca; C-3, 5 wt.% Ca; C-4, 7 wt.% Ca; C-5, 5 wt.% Fe and C-6, pure activated carbon).

The electrochemical characteristics of the DC-SOFCs operated on 1 wt. %, 3 wt. %, 5 wt. %, 7 wt. % Ca-loaded activated carbon, 5 wt. % Fe-loaded activated carbon and pure activated carbon are shown in Fig. 5 and listed in Table 1. Because of the identical

fabricating technique for preparing the cells and operating temperature, the performance difference of the cells should be attributed to the difference of carbon fuel. As shown in Table 1, the performances of the DC-SOFCs operated on the carbon fuels loaded with catalyst, including Ca and Fe, are significantly higher than that with pure carbon fuel (258 mW cm^{-2}), indicating that loading catalyst on carbon fuel is an effective way to improve the output performance, which has been demonstrated by Tang and Liu from our group [18]. For comparison, 5 wt. % Ca-loaded activated carbon DC-SOFC gives a peak power density of 373 mW cm^{-2}, which is even higher than that fueled by 5 wt. % Fe-loaded activated carbon (352 mW cm^{-2}), indicating that Ca exhibits good catalytic effect for Boudouard reaction. What's more, the power densities and OCVs of Ca-loaded activated carbon DC-SOFCs are improved with increasing Ca content from 1 wt. % to 7 wt.%. However, as shown in Table 1, performance difference between 5 wt. % and 7 wt. % Ca content is negligible. In other words, when Ca content is over 5 wt. %, the cell performance improvement is limited. The performances of the DC-SOFCs with Ca-loaded carbon fuel are also significantly higher than the result of Li et. al. (about 150 mW cm^{-2} at 850 ºC with 10 wt. % Ca loading content) [30], which might due to the totally different cell configuration, carbon phases and Ca loading content. Fig. 5 (b) reveals the electrochemical impedance spectra of the DC-SOFCs measured under open circuit voltage. The ohmic resistances of all the cells are almost the same (0.54 Ω cm^2) due to the identical operating temperature and SOFC configuration. However, the polarization resistances of the cells are different. The

lowest polarization resistance is attributed to the 7 wt. % Ca-loaded activated DC-SOFC and the highest polarization resistance is attributed to the pure activated carbon one. It is reasonable that the DC-SOFC operated on the pure activated carbon gives the largest polarization resistance, because the Boudouard reaction (2) rate might be too slow to provide sufficient CO for the electrochemical reaction (1), which also decreases the OCV. Generally, the resistance of a cell under discharging conditions is higher than that under OCV. However, in our experiment, the increased amount of resistance between OCV and discharging conditions is so small that it could be neglected, because of the high linearity of the I-V curves. The better performance and lower polarization resistance of the Ca-loaded activated carbon DC-SOFC than those of the DC-SOFC operated on Fe-loaded activated carbon suggests that the Boudouard reaction on the Ca-loaded activated carbon is better catalyzed than that on the other one, which has been demonstrated before. Huang et al. [31] studied the catalytic effect of alkali (K and Na), alkaline earth (Ca and Mg) and transition (Fe) metals on the Boudouard reaction of fir char and found that catalytic reactivity of the metals in the order of K > Na > Ca > Fe > Mg. Similarly, Lahijani et al. [32] investigates the influence of alkali (K and Na), alkaline earth (Ca and Mg) and transition (Fe) metal nitrates on CO_2 gasification reactivity of pistachio nut shell char. The results shows the catalytic reactivity in the order of Na > Ca > Fe > K > Mg.

These results support our conclusion that the catalytic activity of Ca is even better than that of Fe. However, to further demonstrate the above conclusion, the reactivity of

all the catalyst-loaded carbon fuel in the experiment is investigated under programmed-temperature conditions using a Thermogravimetric analyzer. Carbon conversion (x) is calculated using the following equation:

$$x = \frac{w_0 - w_t}{w_0 - w_r} \quad (3)$$

where w_0 is the initial mass of the char at the start of gasification, w_t is the mass at gasification time t, and w_r is the mass of ash and catalyst remaining after complete gasification. The carbon conversion of carbon fuel with different loading of catalyst is showed in the following figure (Fig. 6):

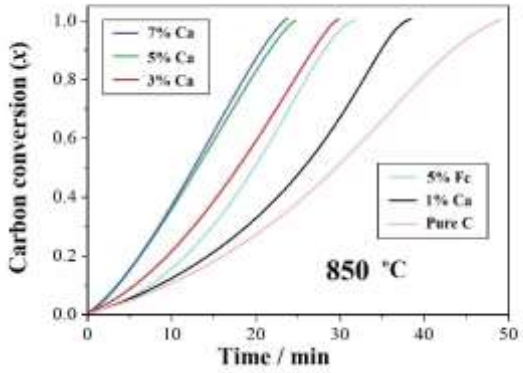

Fig. 6 - Carbon conversion of different catalyst-loaded carbon fuel at 850 ºC.

As shown in Fig. 6, the gasification reactivity of carbon fuel enhances with the increasing loading content of Ca. However, carbon conversion rate of 7 % Ca-loaded carbon fuel is almost the same as that of 5 % Ca-loaded carbon, which further explains the results of the corresponding SOFC performances. The catalytic activity of Ca is higher than that of Fe with the same loading content. Such observation is in agreement with the results of Huang and Lahijani [31, 32].

Both Fe and Ca are very effective catalysts to the Boudouard reaction. However, they are not necessarily better than any other metal oxides. For example, the transition metal Co is also a good catalyst for the Boudouard reaction, but its cost is much higher than that of Fe. Similarly, Ca oxide is the most inexpensive among the alkaline earth metal oxides. Meanwhile, the catalytic activity of Fe and Ca are comparable to that of the other transition metal and alkaline earth metal. Therefore, Fe and Ca are loaded on the carbon fuel of DC-SOFCs to promote the Boudouard reaction for producing sufficient CO to the redox reaction of the anode. In general, the mechanism of metal catalytic carbon gasification can be described by the "spill-over" model [33]. Firstly, CO_2 adsorbs and dissociates on a metal catalyst to form a metal catalyst-CO_2 complex. Secondly, the complex migrate to nearby carbon substrate to react with carbon, producing two CO molecules. For Ni catalyst, C dissolves and diffuses in nickel metal, and the carbon gasification takes place on the surface of the Ni metal-gas interface. For Fe catalyzed carbon fuel, carbon gasification can be described using the following model [34]:

$$Fe_nO_m + CO_2 = Fe_nO_{m+1} + CO \quad (4)$$

$$Fe_nO_{m+1} + C = Fe_nO_m + CO \quad (5)$$

where *n* and *m* represent different form of Fe catalyst, because Fe catalyst could be Fe_2O_3, FeO, Fe_3O_4 and Fe metal under different operating conditions [35]. The reaction rate-determining step is $Fe_nO_{m+1} + C = Fe_nO_m + CO$.

For the Ca catalyzed carbon gasification, CaO is highly active on chemisorption

of CO_2 and further to form $CaCO_3$, followed by the solid-state reaction between $CaCO_3$ and carbon. The mechanism is described as the following model [36]:

$$CaO + CO_2 = CaCO_3 \quad (6)$$

$$CaCO_3 + C = CaO + 2CO \quad (7)$$

In this model, reaction (7) is the reaction rate-determining step. To gasify carbon at the external surface, a catalyst particle must solubilize it at the internal surface. To solubilize carbon atoms there must be active contact with carbon. To have active contact a "sintering-like" faceting of the particle is required. [37] Therefore, Tammann temperature (at which lattices begin to be appreciably mobile) is an important physical condition to evaluate the catalytic activity of a metal oxide on the Boudouard reaction. Actually, the Tammann temperatures of $CaCO_3$ (533 K) and Fe oxides (FeO (552 K), Fe_2O_3 (633 K), Fe (632 K)) are much lower than that of other metal oxides, such as MgO (1562 K), Cr_2O_3 (1081 K), V_2O_3 (833 K). Benefited from a low Tammann temperature, Fe and Ca exhibit such good catalytic properties for the Boudouard reaction.

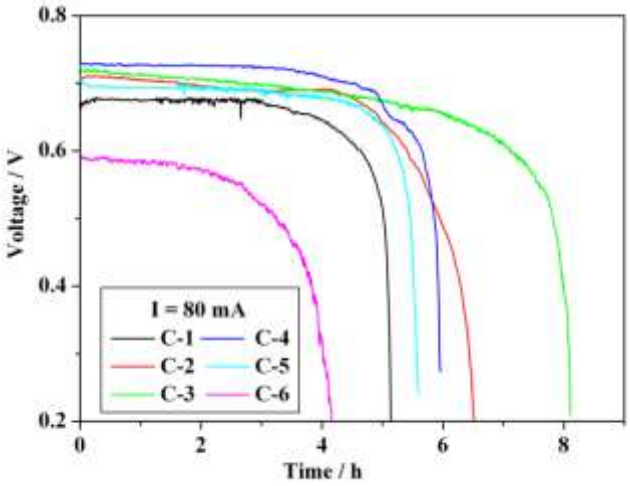

321

322 **Fig. 7 – The discharging curves of DC-SOFCs with C-1 to C-6 fuels,**

323 **respectively, operated at constant current (80 mA), at 850 ºC.**

324

325

326 **Table 2 – The discharging times and fuel utilization of DC-SOFCs with C-1 to C-**

327 **6 carbon fuels.**

	C-1	C-2	C-3	C-4	C-5	C-6
Catalyst	1 % Ca	3 % Ca	5 % Ca	7 % Ca	5 % Fe	none
Discharging time/ h	5.15	6.53	8.11	5.96	5.60	4.40
Fuel utilization/ %	11.5	14.6	18.2	13.4	12.6	9.9

328

329 Fig. 7 is the discharging curves of the DC-SOFCs with a variety of carbon

330 fuels at 850 ºC and at a constant current of 80 mA (364 mA cm^{-2}). Under constant

331 discharging current of 80 mA, the variation trend of the discharging plateaus of

332 all the DC-SOFCs is consistent with that of the I-V-P curves. The discharging

333 times and corresponding fuel utilizations of the DC-SOFCs with the six carbon
334 fuels are listed in Table 2. Apparently, The C-3 (5 wt. % Ca-loaded activated
335 carbon) cell achieves the longest discharging time of 8.11 h, with a discharging
336 plateau significantly higher than that of C-6 (pure activated carbon, 4.40 h) cell
337 and C-5 (5 wt. % Fe-loaded activated carbon, 5.60 h) cell. The above results
338 demonstrate that loading a suitable amount of Ca on activated carbon can
339 promote the discharging time and fuel utilization of a DC-SOFC, which is
340 comparable to a Fe-loaded activated carbon. For the cell with C-4 fuel (7 wt. %
341 Ca-loaded activated carbon), the total test time is reduced to 5.96 h. As the
342 Boudouard reaction catalyst, Ca is distributed on the carbon fuel in form of CaO,
343 which tends to agglomeration and caking. Therefore, CaO might be
344 agglomerated when the amount of Ca increases to 7 wt. %, and further impacts
345 on the catalytic effect of Boudouard reaction and the discharging time of a DC-
346 SOFC. Moreover, the operated temperature is as high as 850 ºC, which might
347 further promote the agglomeration of CaO. To demonstrate this conclusion, the
348 microstructures and element distribution are characterized through SEM and
349 EDX. As shown in Fig. 8 (a) and (b), the particles of the 7 wt. % Ca-loaded
350 activated carbon are highly porous, with an average particle size of about 20 μm.
351 EDX measurement on the surface of a particle shows that there is a small amount
352 of Ca (3.84 wt. %) distributed on the surface, as shown in Fig.8 (c). However,
353 after a cell operation of 80 mA at 850 ºC, some larger agglomerates are formed,

as shown in Fig.8 (d) and (e). Fig.8 (f) shows an EDX analysis for the surface of such an agglomerate. As it shows, the weight percentage of Ca, C, and O is 38.28, 14.62, and 47.10, respectively. A mole ratio of Ca: C: O=1:1.25:3 is obtained based on these values. Thus it is reasonable to assume that Ca exists in the form of $CaCO_3$.

The particle size and distribution of Ca catalyst are further measured by a laser particle size analyzer (LA-960 Laser Particle Analyzer, Horiba Scientific, Japan). Firstly, the 7 wt. % Ca-loaded carbon fuel before and after cell operation are fired in an oxygen atmosphere at 350 ºC, respectively, to consume carbon and get Ca catalyst powders. Then the Ca catalyst powders are collected to measure particle size. The particle size distributions are shown in Fig. S2 in the supplementary material. Apparently, after cell operation, the particle size of Ca catalyst grows significantly from a distribution range of 0.1-10 μm to 1-60 μm. The average particle size of Ca catalyst before cell operation is 4.7 μm, and increases to 27.2 μm after cell operation, indicating that Ca catalyst powder particle is significantly grown and agglomerated under cell operation.

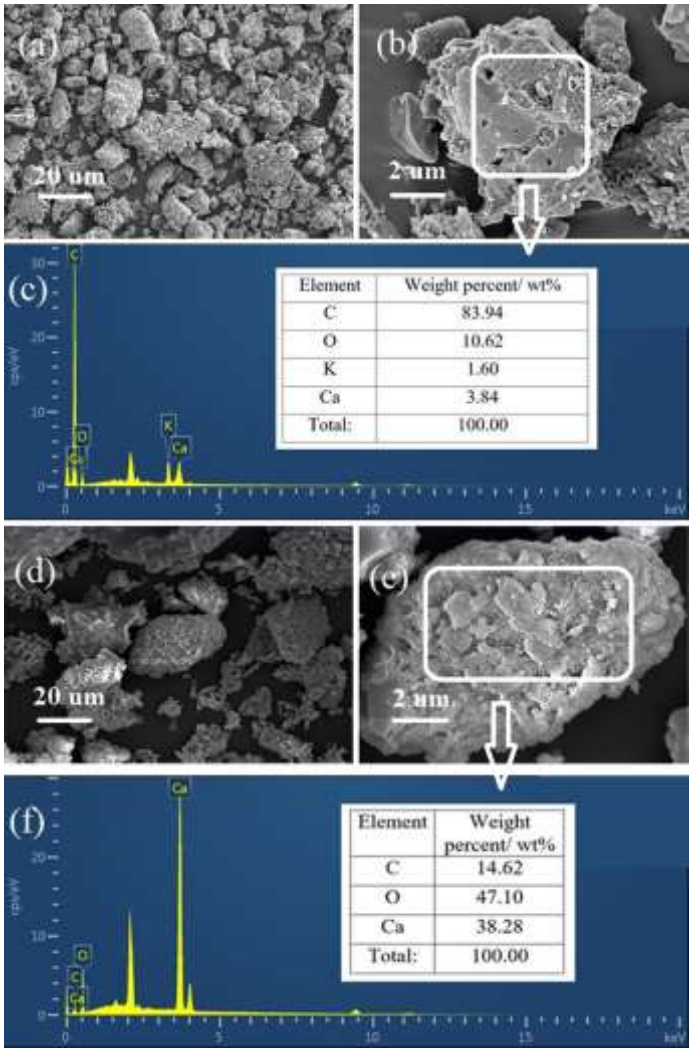

Fig. 8 - SEM pictures of 7 wt. % Ca-loaded activated carbon before (a and b) and after (d and e) cell operation, with corresponding element distribution diagrams (c and f).

In fact, a sintering process of carbon containing calcium is found when it is under prolonged thermal treatments or gasified to burn-off levels in CO_2 atmosphere [38]. Furthermore, the Ca catalyst reactivity decreases remarkably with the sintering process, because of the drop in the available surface area of Ca catalyst and contact area between Ca and C. Therefore, the agglomeration and

sintering of Ca catalyst might be the main reason for the reduced fuel utilization of DC-SOFC.

From Table 2, the total discharging time of C-3 cell is 8.11 h, at a constant discharge current of 80 mA. During the discharging test, there is 2336 C charge delivered, indicating that 0.072 g of carbon has been oxide through electrochemical reaction, calculating base on the overall reaction of the cell as $C + 2O^{2-} = CO_2 + 4e^-$ (4 electrons reaction). Therefore, the carbon fuel utilization of C-3 cell is 18.2 %, as 0.4 g carbon has been loaded into each DC-SOFC. Due to the longest discharging time, the C-3 cell gives the highest fuel utilization among all the cells, which is 45 % higher than that of the C-5 (5 % Fe-loaded activated carbon) cell. This is a further indication of the advantages of the Ca-loaded activated carbon for DC-SOFCs.

4. Conclusions

A Ca-loaded activated carbon is proved to be an excellent carbon fuel for DC-SOFCs. DC-SOFCs operated on solid carbon fuel loading with different Ca amount are tested. It is found that 5 wt. % Ca-loaded activated carbon is the most favoured carbon fuel for DC-SOFC, as the cell powered by 5 wt. % Ca-loaded activated carbon gives the maximum power density of 373 mW cm^{-2}, at 850 ºC, even slightly higher than that operated on the best reported 5 wt. % Fe-loaded activated carbon (352 mW cm^{-2}), and much larger than that of the cell with pure

carbon (258 mW cm^{-2}). Moreover, the fuel utilization of the DC-SOFC, operated at a constant discharging current of 80 mA and a cell voltage of about 0.7 V, with the 5 wt. % Ca-loaded carbon fuel is the highest among the six kinds of cell. With the same discharging current and higher discharging voltage, the cell with 5 wt. % Ca-loaded activated carbon exhibits 45 % larger discharging time and fuel utilization than that of the cell with Fe-loaded carbon fuel. However, when the amount of Ca increases from 5 wt. % to 7 wt. %, the discharging time and fuel utilization of the cell reduce to 73 %, with a limited superior output performance. SEM and particle size distribution of 7 wt. % activated carbon fuel demonstrated that the reduced fuel utilization might due to the agglomeration and sintering of Ca catalyst. All in all, comparing to the conventional Fe-loaded carbon, Ca-loaded carbon for DC-SOFCs has the advantages of lower cost, higher output performance and fuel utilization. It is a promising catalyst to load on carbon fuels for DC-SOFC.

Acknowledgements

This work was supported by the National Science Foundation of China (NSFC, No. 21276097), the Special Funds of Guangdong Province Public Research and Ability Construction (No. 2014A010106008), Guangdong Innovative and Entrepreneurial Research Team Program, Program of Excellent Ph. D Thesis Authors of Guangdong Province, and a fund from Environmental Conservation Fund of Hong Kong SAR (ECF 54/2015). Sincere thanks to Yongmin Xie, Jie Xiao and Yubao Tang for helpful discussion.

References

[1] Shafiee S, Topal E. When will fossil fuel reserves be diminished. Energy Policy 2009; 37: 181-9.

[2] Muhammad A, Muneer T. Energy supply, its demand and security issues for developed and emerging economies. Renew Sust Energy Rev 2007; 11: 1388-413.

[3] Nabae Y, Pointon KD, Irvine JTS. Electrochemical oxidation of solid carbon in hybrid DCFC with solid oxide and molten carbonate binary electrolyte. Energy Environ Sci 2008; 1: 148-55.

[4] Cao D, Sun Y, Wang G. Direct carbon fuel cell: Fundamentals and recent developments. J Power Sources 2007; 167: 250-7.

[5] Hemmes K, Cooper JF, Selman JR. Recent insights concerning DCFC development: 1998–2012. Int J Hydrogen Energy 2013; 38: 8503-13.

[6] Cherepy NJ, Fiet KJ, Krueger R, Jankowski AF, Cooper JF. Direct Conversion of

Carbon Fuels in a Molten Carbonate Fuel Cell. J Electrochem Soc 2004; 152: A80-7.

[7] Jain SL, Nabae Y, Lakeman BJ, Pointon KD, Irvine JTS. Solid state electrochemistry of direct carbon/air fuel cells. Fuel Cells Bull 2008; 179: 1417-21.

[8] Jain SL, Lakeman JB, Pointon KD, Marshall R, Irvine JTS. Electrochemical performance of a hybrid direct carbon fuel cell powered by pyrolysed MDF. Energy Environ Sci 2009; 2: 687-93.

[9] Pointon K, Lakeman B, Irvine J, Bradley J, Jain S. The development of a carbon–air semi fuel cell. J Power Sources 2006; 162: 750-6.

[10] Gür TM, Huggins RA. Direct Electrochemical Conversion of Carbon to Electrical Energy in a High Temperature Fuel Cell. J Electrochem Soc 1992; 139: L95-7.

[11] Jiao Y, Tian W, Chen H, Shi H, Yang B, Li C, et al. In situ catalyzed Boudouard reaction of coal char for solid oxide-based carbon fuel cells with improved performance. Appl Energy 2015; 141: 200-8.

[12] Cooper JF. Direct Conversion of Coal and Coal-Derived Carbon in Fuel Cells. ASME 2004 2nd International Conference on Fuel Cell Science, Engineering and Technology, American Society of Mechanical Engineers. 2004; p. 375-85.

[13] Heydorn B, Crouch-Baker S. Direct carbon conversion: progressions of power. Fuel Cell Review 2006; 15.

[14] Li X, Zhu Z, Marco RD, Bradley J, Dicks A. Evaluation of raw coals as fuels for direct carbon fuel cells. J Power Sources 2010; 195: 4051-8.

461 [15] Giddey S, Badwal SPS, Kulkarni A, Munnings C. A comprehensive review of
462 direct carbon fuel cell technology. Prog Energy Combust Sci 2012; 38: 360-99.
463 [16] Nakagawa N, Ishida M. Performance of an internal direct-oxidation carbon fuel
464 cell and its evaluation by graphic exergy analysis. Ind Eng Chem Res 1988; 27:
465 1181-5.
466 [17] Tang Y, Liu J, Sui J. A Novel Direct Carbon Solid Oxide Fuel Cell. Ecs Trans 2009;
467 25: 1109-14.
468 [18] Tang Y, Liu J. Effect of anode and Boudouard reaction catalysts on the performance
469 of direct carbon solid oxide fuel cells. Int J Hydrogen Energy 2010; 35: 11188-93.
470 [19] Tang Y, Liu J. Fueling Solid Oxide Fuel Cells with Activated Carbon. Acta Phys-
471 Chim Sin 2010; 26: 1191-4.
472 [20] Bai Y, Yan L, Tang Y, Xie Y, Liu J. Direct carbon solid oxide Fuel Cell—a potential
473 high performance battery. Int J Hydrogen Energy 2011; 36: 9189-94.
474 [21] Xie Y, Tang Y, Liu J. A verification of the reaction mechanism of direct carbon
475 solid oxide fuel cells. J Solid State Electrochem 2013; 17: 121-7.
476 [22] Cai W, Zhou Q, Xie Y, Liu J. A facile method of preparing Fe-loaded activated
477 carbon fuel for direct carbon solid oxide fuel cells. Fuel 2015; 159: 887-93.
478 [23] Yu X, Shi Y, Wang H, Cai N, Li C, Ghoniem AF. Using potassium catalytic
479 gasification to improve the performance of solid oxide direct carbon fuel cells:
480 Experimental characterization and elementary reaction modeling. J Power Sources
481 2014; 252: 130-7.

[24] Wu Y, Su C, Zhang C, Ran R, Shao Z. A new carbon fuel cell with high power output by integrating with in situ catalytic reverse Boudouard reaction. Electrochem Commun 2009; 11: 1265-8.

[25] Skrzypkiewicz M, Lubarska-Radziejewska I, Jewulski J. The effect of Fe2O3 catalyst on direct carbon fuel cell performance. Int J Hydrogen Energy 2015; 40: 13090-8.

[26] Cai W, Liu J, Xie Y, Xiao J, Liu M. An investigation on the kinetics of direct carbon solid oxide fuel cells. J Solid State Electrochem 2016; 20: 2207-16.

[27] Feighery AJ, Irvine JTS. Effect of alumina additions upon electrical properties of 8 mol.% yttria-stabilised zirconia. Solid State Ionics 1999; 121: 209-16.

[28] Lei L, Bai Y, Liu J. Ni-based anode-supported Al_2O_3-doped-Y_2O_3-stabilized ZrO_2 thin electrolyte solid oxide fuel cells with Y_2O_3-stabilized ZrO_2 buffer layer. J Power Sources 2014; 248: 1312-9.

[29] Wang F-Y, Cheng S, Wan B-Z. Porous Ag–CGO cermets as anode materials for ITSOFC using CO fuel. Catal Commun 2008; 9: 1595-9.

[30] Chen L, Shi Y, Cai N. Performance improvement of direct carbon fuel cell by introducing catalytic gasification process. J Power Sources 2010; 195: 4660-6.

[31] Huang Y, Yin X, Wu C, Wang C, Xie J, Zhou Z, et al. Effects of metal catalysts on CO 2 gasification reactivity of biomass char. Biotechnol Adv 2009; 27: 568-72.

[32] Lahijani P, Zainal ZA, Mohamed AR, Mohammadi M. CO_2 gasification reactivity of biomass char: catalytic influence of alkali, alkaline earth and transition metal

503 salts. Bioresour Technol 2013; 144: 288-95.
504 [33] Tomita A. Catalysis of carbon–gas reactions. Catalysis Surveys from Japan 2001;
505 5: 17-24.
506 [34] Furimsky E, Sears P, Suzuki T. Iron-catalyzed gasification of char in CO2. Energy
507 & fuels 1988; 2: 634-9.
508 [35] McKee DW. Effect of metallic impurities on the gasification of graphite in water
509 vapor and hydrogen. Carbon 1974; 12: 453-64.
510 [36] Taylor HS, Neville HA. Catalysis in the intereation of carbon with steam and with
511 carbon dioxide. J Am Chem Soc 1921; 43: 2055-71.
512 [37] Lobo LS, Carabineiro SA. Kinetics and mechanism of catalytic carbon gasification.
513 Fuel 2016; 183: 457-69.
514 [38] Cazorla-Amorós D, Linares-Solano A, De Lecea CS-M, Joly J. Calcium-carbon
515 interaction study: its importance in the carbon-gas reactions. Carbon 1991; 29: 361-
516 9.
517
518
519
520
521
522
523 # Figure captions

Fig. 1–Schematic diagram of a DC-SOFC.

Fig. 2 – SEM pictures of cross-section (a, scale: 300) and anode (b, scale: 1000) of the as prepared SOFC.

Fig. 3 – The output performance plot with error bars (a) and impedance spectra (b) of a typical as-prepared SOFC operated at 850 ºC using H_2 as fuel gas.

Fig. 4 – SEM image (a) and EDX diagrams of the Ca-loaded activated carbon fuel (5 wt. %) on different sites.

Fig. 5 – I-V-P characteristics (a) with error bars and impedance spectra (b) of the SOFCs operated at 850 ºC using the different kinds of catalyst-loaded carbon fuel (C-1, 1 wt.% Ca; C-2, 3 wt.% Ca; C-3, 5 wt.% Ca; C-4, 7 wt.% Ca; C-5, 5 wt.% Fe and C-6, pure activated carbon).

Fig. 6 - Carbon conversion of different catalyst-loaded carbon fuel at 850 ºC.

Fig. 7 – The discharging curves of DC-SOFCs with C-1 to C-6 fuels, respectively, operated at constant current (80 mA), at 850 ºC.

Fig. 8 - SEM pictures of 7 wt. % Ca-loaded activated carbon before (a and b) and after (d and e) cell operation, with corresponding element distribution diagrams (c and f).